Imaging fracture permeability using magnetotellurics

Alison Kirkby*
University of Adelaide, North Terrace, Adelaide 5005
Geoscience Australia, Symonston, ACT 2609
Alison.Kirkby@adelaide.edu.au

Graham Heinson
University of Adelaide
North Terrace, Adelaide 5005
Graham.Heinson@adelaide.edu.au

Simon Holford
University of Adelaide
North Terrace, Adelaide 5005
Simon.Holford@adelaide.edu.au

SUMMARY

We present 1D anisotropic inversions of magnetotelluric data in two regions of the Otway Basin; Koroit, Victoria, and Penola, South Australia. In the Koroit region we have delineated an electrically anisotropic layer at approximately 2.5 to 3.5 km depth; this corresponds to the upper part of the Lower Cretaceous Crayfish Group, a known reservoir unit. The anisotropy strike is consistent between stations at approximately 160° east of north. We interpret the anisotropy at Koroit as resulting from pervasive NNW oriented, fluid-filled fractures, resulting in enhanced bulk electrical and hydraulic conductivity. This interpretation is consistent with permeability data from well formation tests. It is also consistent with the orientation of mapped faults in the area, which are favourably oriented for reactivation in the current stress field. In Penola, no persistent anisotropic layer has been defined even though the areas are geologically similar. The difference in the resistivity structure may reflect differences in the density of fractures or their fill material. Alternatively, it may reflect small differences in the amount by which the fractures are open, resulting from differences in the stress field and fracture orientation in each area.

Key words: resistivity, permeability, fractures, fluids

INTRODUCTION

The ability to predict the crustal permeability distribution is important for resources industries such as geothermal, where high permeability is vital to the ability to extract heat at an adequate rate for commercial production. Likewise, in the oil and gas industry, knowledge of the permeability is important, both in accurately identifying potential hydrocarbon traps, and in predicting reservoir potential (e.g., Babadagli & Al-Salmi 2004).

Electromagnetic techniques are widely used in the exploration of conventional geothermal targets (e.g., Pellerin et al. 1996; Muñoz 2014), where the target is a low resistivity anomaly resulting from high temperature alteration of the host rock to form clay minerals (Wright et al. 1985; Ussher et al. 2000). However, unconventional geothermal targets are located in a range of different geological settings (e.g. Barnett & Evans 2010; de Graaf et al. 2010). The application of electromagnetic techniques such as magnetotellurics (MT) in such settings may be less straightforward.

Time lapse MT monitoring of an enhanced geothermal system near Paralana, South Australia was performed in 2011 (Peacock et al. 2012, 2013; MacFarlane et al. 2014). In this experiment, MT data were collected pre- and post-injection of an electrically conductive fluid into a natural fault network at 3.6 km depth. Much stronger increases in electrical conductivity were observed parallel to the strike of the fault network than perpendicular to it, consistent with an increase in hydraulic conductivity. These observations show that the addition of a conductive fluid to a fracture network can change the conductivity, and that this is measurable from the surface.

The primary data type used for exploration of reservoir properties in the oil and gas industry is seismic reflection (e.g., Russell et al. 1997; Hart & Balch 2000). Seismic and well log data are used to infer properties such as porosity and water saturation. Seismic attribute mapping has been used to map fractures and faults in several areas across Australia, including the Penola Trough of the Otway Basin (Bailey et al. 2014). While electromagnetic techniques are less commonly applied in hydrocarbon exploration, electrical resistivity logs are sometimes used to derive porosity through Archie's Law (Archie 1942).

The Otway Basin has long been a target for petroleum exploration, with the first commercial discovery in 1987 (O'Neil 2002). As a result, considerable seismic and well data exist across the basin, and these data have been used to characterise the regional structure and stress field (e.g., Hillis et al. 1995; Vandenberg 2000; Nelson et al. 2006). More recently, the Otway Basin has been of interest for geothermal energy, with exploration occurring near Koroit, Victoria and in the Penola Trough (Figure 1; Barnett & Evans 2010; de Graaf et al. 2010).

In 2008, an MT dataset was collected for Hot Rock Ltd to identify the distribution of heat and fluids near Koroit. Strong resistivity and phase splits are observed in these data, and these have been interpreted as resulting from macro scale electrical anisotropy resulting from the presence of fractures and faults. This work was presented in detail by Kirkby et al. (2015) and is summarised in this paper. More recently, an MT dataset was collected in the Penola Trough region of the Otway Basin, coincident with the Haselgrove–Balnaves 3D seismic survey. These data are also presented here.

THE OTWAY BASIN

The Otway Basin covers southern Victoria, South Australia and extends offshore towards Tasmania (Figure 1). The basin is broadly WNW trending, and developed along the Australian southern margin as a result of Jurassic to Cretaceous rifting and separation of the Australian continent from Antarctica (Perincek & Cockshell 1995). Sedimentation commenced with the deposition of the Casterton Formation, followed by the Crayfish Group in the Early Cretaceous. Deposition of the Crayfish Group was followed by a period of uplift, tilting and erosion in the mid-Cretaceous, leaving an unconformity at the top of the Crayfish Group. The current stress field in the Otway Basin is reverse to strike-slip, with the maximum horizontal stress oriented at approximately 135° (Hillis et al. 1995; Nelson et al. 2006; Tassone 2014).

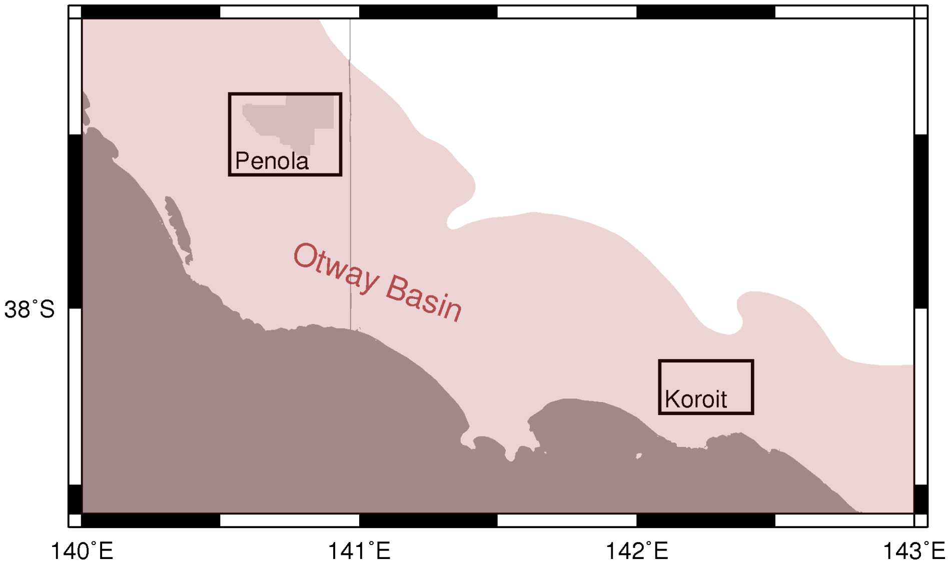

Figure 1. Map showing the locations of the Penola and Koroit regions of the Otway Basin. Otway Basin extent shown in pink.

Deposition of the Crayfish Group was concentrated in a series of W to NW trending depocentres that extend across the Otway Basin (Perincek & Cockshell 1995). These depocentres include the Tyrendarra Embayment in the Koroit region, an approximately west trending half graben in the central Otway Basin, and the Penola Trough in the western Otway Basin (Perincek & Cockshell 1995). The orientation of the depocentres cross-cuts the NNW orientation of basement fabric in the Delamerian Fold Belt, which underlies the Otway Basin in the Koroit region (Vandenberg 2000).

Sediments of the Crayfish Group have been targeted as reservoirs for both oil and gas and geothermal prospects, due to their high permeability (Morton et al. 2002; Barnett & Evans 2010; de Graaf et al. 2010). In the Penola Trough, the Crayfish Group has been divided into the Pretty Hill Formation and the overlying Laira Formation and Katnook Sandstone (Boult et al. 2002). However, this subdivision is much less clear within the Tyrendarra Embayment (Ryan et al. 1995).

THE MAGNETOTELLURIC METHOD

The magnetotelluric (MT) method is a passive geophysical technique that measures time variations in orthogonal components of the Earth's electrical (**E**) and magnetic (**B**) fields (Tikhonov, 1950; Cagniard, 1953). The measurements provide information on the electrical conductivity structure of the subsurface in the frequency domain. The impedance tensor **Z** is related to the horizontal components of the **E** and **B** fields through the relationship $\mathbf{E} = \mathbf{ZB}$.

The MT phase tensor $\mathbf{\Phi}$ is given by $\mathbf{\Phi} = Re(\mathbf{Z})^{-1}\, Im(\mathbf{Z})$, and can be depicted as an ellipse (Bibby 1986; Caldwell et al. 2004). If the MT data are 1D, the ellipse is a circle. In 2D, the orientation of the ellipse is either parallel or perpendicular to the geoelectric strike. To overcome this ambiguity, the vertical magnetic field information can also be utilised through calculation of induction vectors. Induction vectors are a representation of the complex ratio of the vertical to horizontal magnetic field components. Vertical magnetic fields are induced by lateral variations in conductivity, and therefore induction vectors can be used to infer the presence and direction of lateral conductivity variations.

Because MT is a diffusive technique, resolution decreases with depth of penetration. As a result, features spaced less than 1 to 2 km apart are unlikely to be individually resolved at depths greater than a few kilometres. Instead, such features may be detected as larger scale electrical anisotropy. Electrical anisotropy is the variation in electrical resistivity with orientation (Wannamaker 2005). It is often the result of mixing of different materials with contrasting electrical conductivities, for example fractures filled with an electrically conductive material.

MAGNETOTELLURIC DATA

Figure 2 shows the MT data from the Koroit and Penola regions as phase tensor ellipses for a period of 12.5 s and as resistivity and phase curves for two representative stations in each area. The phase tensor ellipses are different for the two areas, being strongly elliptical by a period of 12.5 s at Koroit, but mostly circular at Penola, with the exception of the NE Penola Trough. This is also reflected in the resistivity and phase curves, in which the Z_{XY} and Z_{YX} resistivity and phase values split earlier and in general, by more than in Koroit.

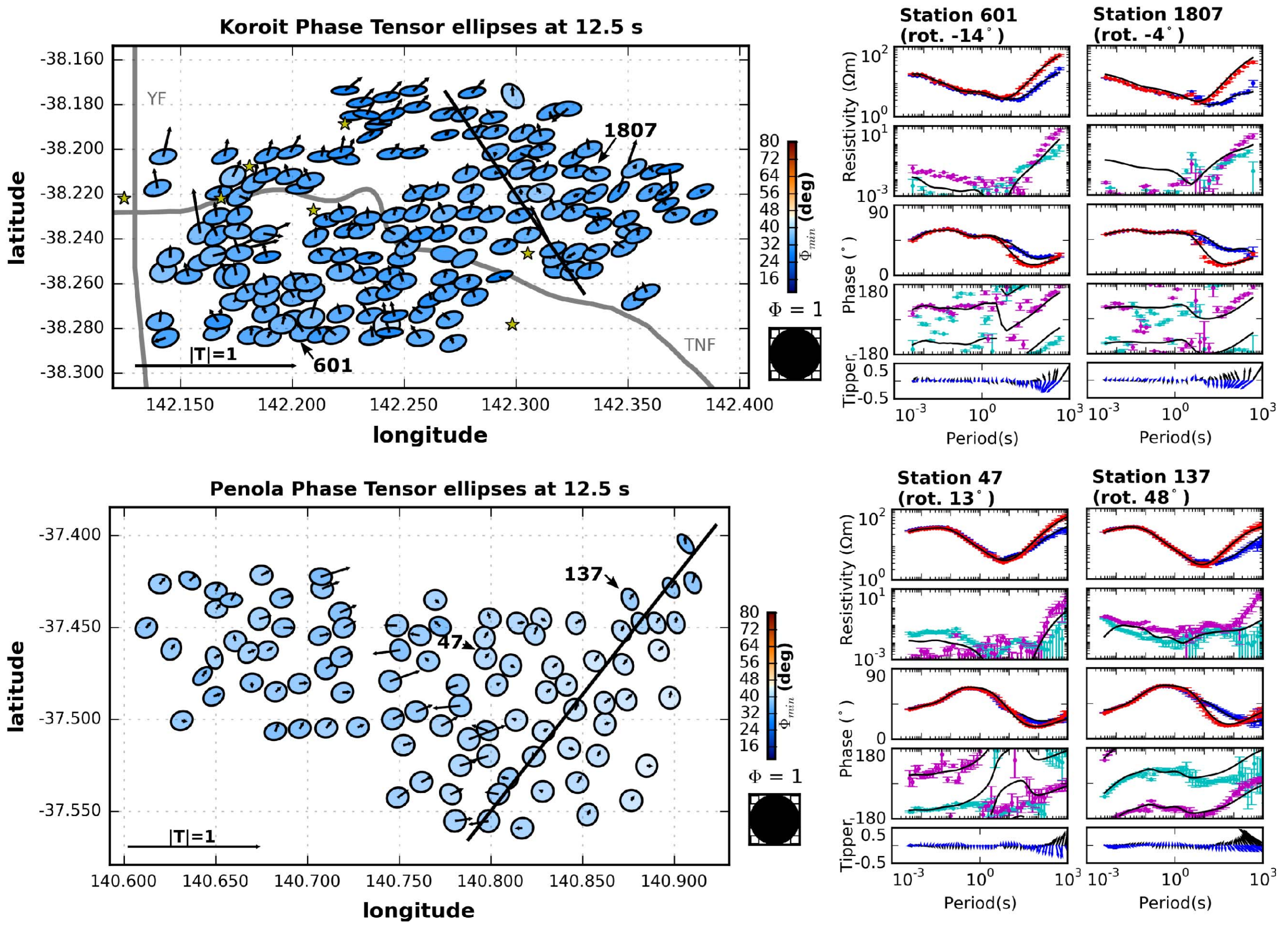

Figure 2. Phase tensor ellipses and induction vectors (plotted using the Parkinson convention) for all stations at a period of 12.5 s, and resistivity and phase curves for all components at two example stations, for Koroit and Penola. Stations have been rotated to strike (calculated as the median strike for periods of 12 to 100 s) to facilitate comparison of the splits in the Z_{XY} (blue) and Z_{YX} (red) resistivity and phase values. Z_{XX} and Z_{YY} resistivity and phase shown in cyan and magenta respectively; real and imaginary induction vectors shown in black and blue respectively. Responses to the unconstrained 1D anisotropic models discussed in this paper at the example stations are shown as black lines.

With the exception of the phase splits, the MT curves are broadly similar between the two regions. In both Penola and Koroit the Z_{XY} and Z_{YX} resistivity and phase are nearly the same to a period of around 10 s indicating 1D structure. The apparent resistivity and phase then decrease with period from about 10 to 30 Ωm at 0.004 s to about 2 to 3 m at about 10 s, and then increase again to 20 to 100 Ωm at the maximum measured period of about 1000 s. One difference between the two regions is that in Penola, the apparent resistivity increases slightly, or remains constant, over periods of 0.004 to 0.1 s before decreasing, whilst in Koroit the apparent resistivity decreases steadily from 0.004 to around 10 s. This suggests there are some more resistive layers in the upper part of the Penola sequence that are not present at Koroit.

MODELLING

Koroit region

The resistivity and phase curves at Koroit indicate the structure is 1D at periods less than 12.5 s. At about 12.5 s, phase splits occur but the induction vectors are small in magnitude up to periods of 50 to 100 s. Furthermore, both the phase tensors and the resistivity structure are very consistent across the array. Therefore, we have interpreted the phase splits in the data as resulting from resistivity anisotropy (Kirkby et al. 2015).

One dimensional anisotropic modelling has been carried out at each station in order to characterise the distribution and amount of anisotropy (Kirkby et al 2015). The inversion algorithm of Pek & Santos (2006) was used to generate smooth 1D anisotropic resistivity models at each station. The algorithm minimises the sum of the model structure, anisotropy, and data-model misfit, and returns the maximum and minimum horizontal resistivity and the anisotropy strike. For the structure penalty values we used the roughness penalty (Constable et al. 1987; Pek & Santos 2006). For the anisotropy penalty we used the ℓ2-norm of the anisotropy.

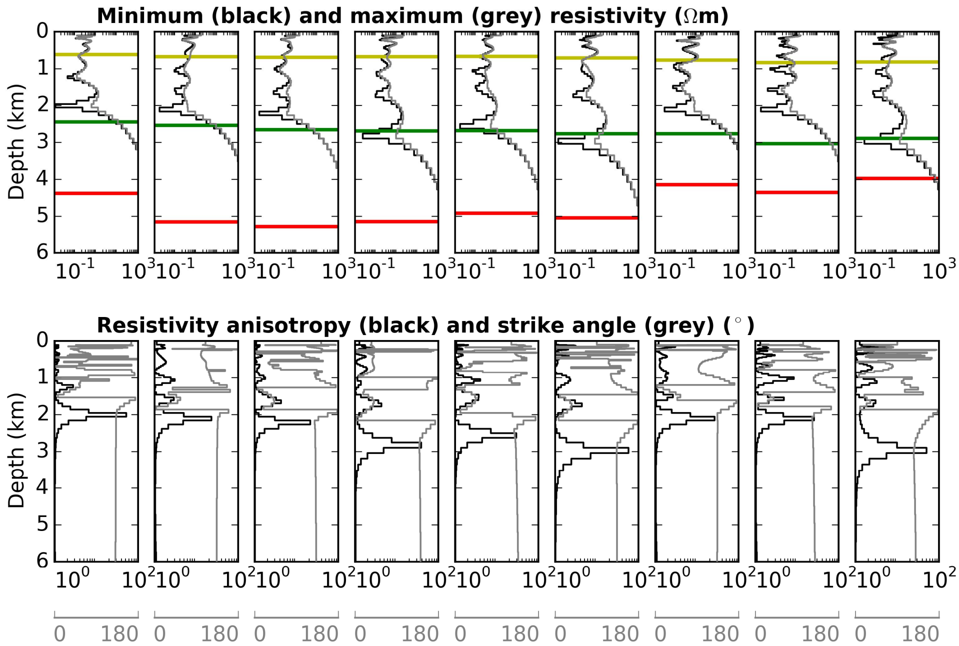

Figure 3. Minimum and maximum resistivity, anisotropy ratio and anisotropy strike from unconstrained 1D anisotropic inversions in the Koroit region. The following stratigraphic horizons are shown as horizontal lines: top Eumeralla Formation (yellow), top Crayfish Group (green), and top Basement (red). Profile locations shown in Figure 2. Stratigraphic horizon interpretations from Hot Rock Ltd. (2009). Modified after Kirkby et al. (2015).

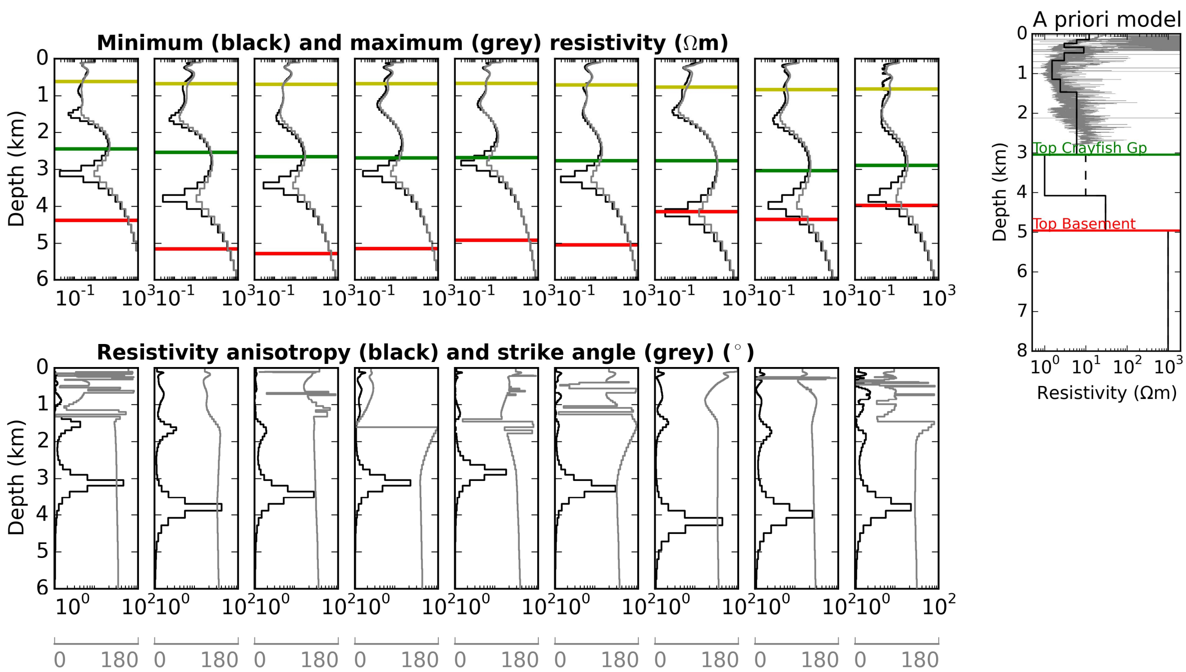

Figure 4. Minimum and maximum resistivity, anisotropy ratio and anisotropy strike from constrained 1D anisotropic inversions in the Koroit region (left) and the *a priori* model (right). Profile locations shown in Figure 2. Stratigraphic horizon interpretations from Hot Rock Ltd. (2009). Modified after Kirkby et al. (2015).

Error floors of 3 % were used for each of the off-diagonal impedence tensor elements. The Z_{XY} and Z_{YX} error values were then used, respectively, as absolute error floors for the Z_{XX} and Z_{YY} elements.

In the inversions, penalty weights can be chosen for both the model roughness and the anisotropy, with higher penalty weights corresponding to smoother and less anisotropic models and (in general) poorer fits to the data, and lower weights corresponding to rougher and more anisotropic models (Pek & Santos 2006). The aim in running the inversions is to find the optimal trade-off between data-model misfit and model roughness. Kirkby et al (2015) carried out an L-curve analysis using several different model runs to select the optimal weights for this dataset, obtaining values of $10^{7.5} \approx 5.6$ for both the anisotropy and roughness penalties.

The resulting inversion models are presented along a NNW-SSE profile in Figure 3, and two example response curves are shown in black in Figure 2. The models generally fit the data well, with a median RMS misfit of 1.7, where the misfit is defined as the ratio of the difference between the data and the model response, and the data error. The inversions reveal an anisotropic layer at approximately 2-3 km, coinciding approximately with the top of the Crayfish Group (Figure 3). We have carried out constrained inversions by providing the inversions with an *a priori* model with anisotropy in the upper Crayfish Group to improve the consistency in the depth of this layer (Figure 4; Kirkby et al. 2015). The inversions were able to follow this *a priori* model closely, whilst maintaining a similar data model misfit to the unconstrained inversions (mean of 1.7). This set of inversions has a median maximum anisotropy ratio of 25, with a median strike of 162° east of north.

Penola region

Similar to Koroit, the MT responses at Penola indicate 1D geoelectric structure at periods less than 12.5 s. However, the phase splits that occur in Penola at around 12.5 s are of much smaller magnitude than at Koroit. Furthermore, the responses are less consistent than at Koroit, with the phase tensor ellipses changing from mostly circular to elliptical in the NE corner of the array. Therefore, if anisotropy is present it is likely to be of smaller magnitude than at Koroit.

Unconstrained 1D anisotropic inversions were carried out at Penola using the same penalty weights as at Koroit but with lower error floors of 1 % of Z_{XY} and Z_{YX}. With these error floors, the mean RMS misfit across the array is 1.5, similar to that at Koroit. A selection of model outputs are presented along a NW–SE oriented profile are presented in Figure 5. The modelled anisotropy magnitudes are much smaller here than at Koroit, reaching maximum values of less than 10 at most stations. The exception is the stations in the NE, where the modelled anisotropy ratio reaches a maximum of 10–30 within basement, similar to the median of the maximum anisotropy at Koroit. However, the NE–SE orientation of the minimum resistivity axis is not consistent with the known orientation of fracture sets from seismic reflection data and borehole image logs (Bailey et al., 2014). Furthermore, the seismic data suggest that both the basement to the Otway Basin, and stratigraphic horizons within the Otway Basin, thin dramatically toward the NE (Figure 5). It is therefore more likely that the phase splits result from larger scale basin structure in the Penola region.

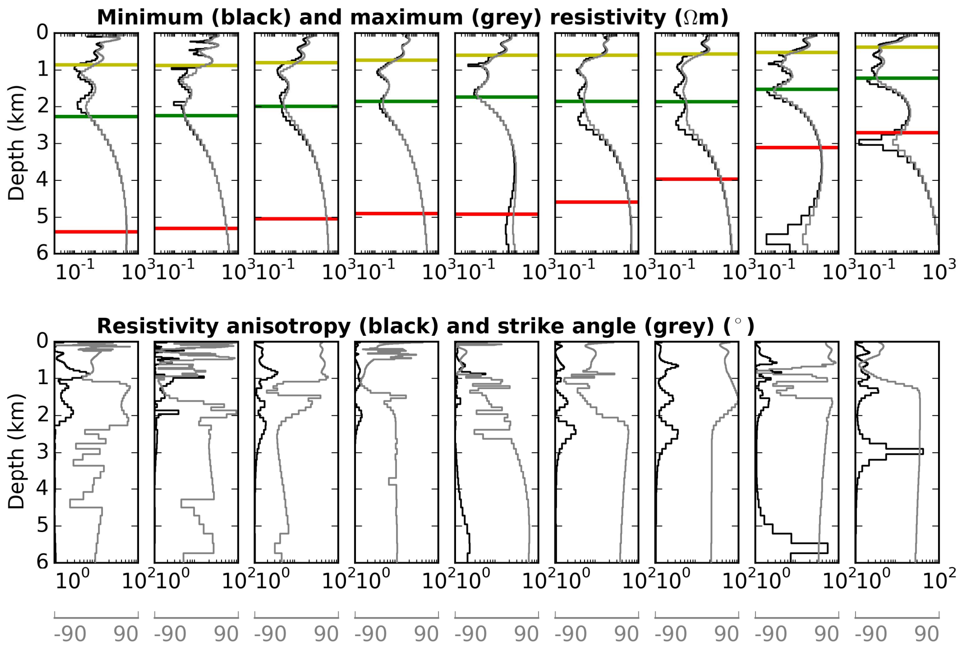

Figure 5. Minimum and maximum resistivity, anisotropy ratio and anisotropy strike from unconstrained 1D anisotropic inversions in the Penola region. Top Eumeralla Formation (yellow) and top Crayfish Group (green) interpreted from the Haselgrove-Balnaves 3D seismic volume. Basement horizon (red) after Jensen-Schmidt et al., 2002. Profile locations shown in Figure 2.

CONCLUSIONS

We have presented 1D anisotropic inversions of MT data from the Koroit and Penola regions of the Otway Basin, Victoria. In the Koroit region, the inversions delineate a persistent anisotropic layer at approximately 2.5 to 3.5 km depth, with an anisotropy strike of about 160 °.

Resistivity anisotropy in the upper crust often results from the mixing of two materials with different electrical conductivities (Wannamaker 2005). Given the shallow sedimentary setting of the datasets, one interpretation of the anisotropy is fractures filled with an electrically conductive material (Kirkby et al. 2015). Because many fractures in the crust are smaller than the resolution of MT at 2.5 to 3.5 km depth, they are unlikely to be individually resolved, but their presence could be observed as bulk anisotropy (Kirkby et al., 2015). Likely fracture fill materials in a shallow sedimentary environment include clay, fluids, or a combination of both. In the Otway Basin, the fluids at about 2 km depth are saline (e.g., Bain 1962; Buckingham 1992), and therefore electrically conductive. Alternatively, Bailey et al. (2014) noted that the electrically conductive mineral siderite was present in some fractures in core samples from the Penola Trough in the western Otway Basin, resulting in them appearing as electrically conductive on image logs. It is possible that siderite is also present in some fractures in the Koroit region. However, structural and stress field data from the Otway Basin are consistent with at least some of the fractures being fluid-filled, as discussed below.

Firstly, permeability data from the wells in the Koroit region and elsewhere show that the Crayfish Group is highly permeable (e.g., Alexander 1992; Morton et al. 2002; Geoscience Australia 2014). In the Koroit region there is only one well where permeability has been measured, Pretty Hill 1. The permeability values measured here is high, ranging from from 200 to 2800 mD, with a median of 600 mD (Geoscience Australia 2014; Geoscience Victoria 2014; Kirkby et al. 2015). Given that the fluids are known to be saline, these high permeability values suggest that the Crayfish Group should be electrically conductive.

Open fractures have been identified in the Crayfish Group in image data from Gordon 1, located 100 km NW of Koroit (3D Geo, 2009). Several electrically conductive fracture sets were identified, including high angle to sub-vertical fractures oriented NNW to NNE. In the Koroit region, there is no image log data available, however 3D Geo (2009) concluded the Crayfish Group was fractured based on dip-meter data in Killara 1. Above the Crayfish Group, the dip is consistent and likely reflects the formation dip (3D Geo, 2009). Within the Crayfish Group, the dip becomes considerably more scattered, which may reflect the influence of fracturing (3D Geo, 2009).

Bailey et al. (2014) analysed the conditions for reactivation of existing faults in the Penola Trough, western Otway Basin, South Australia. The stress field in the Penola Trough is strike-slip with σ_1 oriented at about 125 °. Bailey et al. (2014) generated fracture reactivation susceptibility plots for this stress field for a depth of 3 km. These plots showed that in a strike-slip regime, faults dipping at greater than about 50° and striking between 90 and 165° were most favourably oriented for reactivation. In the central Otway Basin, σ_1 is oriented at 135°, therefore favourable orientations for reactivation should fall within the range 100 to 175°.

In the Koroit region, the basement structural fabric is believed to be oriented NNW (Vandenberg 2000). Based on this fact, the stress field orientation, and the NNW orientation of neotectonic features 100 km to the NE of the Koroit region, Tassone (2014) concluded that recent faulting is being controlled by basement structure.

Thus, the available geological and rock property data in the Koroit region is consistent with a 1D anisotropic interpretation (Kirkby et al., 2015).

In contrast, the anisotropy delineated by the inversions in the Penola region is much weaker at most stations, particularly in the southern and western Penola Trough. In the NE Penola Trough, the modelled anisotropy ratio reaches values of 10 to 30 but the anisotropy strike is not consistent with mapped faults, which have a dominant orientation of NW-SE based on seismic data and borehole image logs. A more likely interpretation is that the MT data are responding to the shallowing of the basin in the NE Penola Trough (Figure 5). Three dimensional MT inversions are being carried out to confirm that this interpretation is able to reproduce the measured responses.

Given that both the Penola Trough and the Koroit region are in the Otway Basin and intersect similar geological units, it is interesting that their MT responses differ so considerably. The difference may reflect differences in the density of fractures, or their dominant fill material, between the two areas. Alternatively, the difference may reflect differences in their susceptibility for reactivation in the present day stress field. Recent numerical modelling of the fluid flow and electrical properties of synthetic fractures has shown that when fractures are close to their percolation threshold, changes in mean aperture of less than 0.1 mm can change the electrical resistivity by a factor of 10 or more, depending on the conductivity of the matrix and fluid (Kirkby et al. 2016). The permeability, on the other hand, can change by several orders of magnitude over this aperture change. Therefore, the subtle differences in the stress field between the Penola Trough and the Koroit region may be sufficient to increase the mean aperture of fractures slightly and thus strongly change the resistivity and permeability that is measured.

ACKNOWLEDGMENTS

We would like to thank Hot Rock Ltd for providing the magnetotelluric data and seismic horizon interpretations used in the Koroit section of this paper. The figures in this extended abstract were generated using GMT, MTPy and other Python plotting libraries.

REFERENCES

3D-Geo, 2009. Hot Rock Ltd, Otway Basin Project, Koroit Geothermal Project, Technical report to Hot Rock Ltd, 3D-GEO.

Alexander, E., 1992. Geology and petrophysics of petroleum reservoirs from the Otway Group, Otway Basin, Tech. Rep. 92/70, Department of Mines and Energy South Australia.

Archie, G., 1942. The electrical resistivity log as an aid in determining some reservoir characteristics, Petroleum Transactions of the Australian Institute of Mining, Metallurgical, and Petroleum Engineers, 146, 54–62.

Babadagli, T. & Al-Salmi, S., 2004. A review of permeability-prediction methods for carbonate reservoirs using well-log data, SPE Reservoir Evaluation & Engineering, 7(02), 75–88.

Bailey, A., King, R., Holford, S., Sage, J., Backe, G., & Hand, M., 2014. Remote sensing of subsurface fractures in the Otway Basin, South Australia, Journal of Geophysical Research, 119, 6591–6612.

Bain, J., 1962. Pretty Hill 1, southwest Victoria, Well Completion Report, Tech. Rep. 7200-G-94, Frome - Broken Hill Company Pty. Ltd.

Barnett, P. & Evans, T., 2010. Exploration and assessment of Hot Sedimentary Aquifer (HSA) geothermal resources in the Otway Basin Victoria, in Proceedings of the 2010 Australian Geothermal Energy Conference, Record 2010/35, pp. 106–111, Geoscience Australia.

Bibby, H. M., Caldwell, T. G., & Brown, C., 2005. Determinable and non-determinable parameters of galvanic distortion in magnetotellurics, Geophysical Journal International, 163(3), 915–930.

Boult, P., White, M., Pollock, R., Morton, J., Alexander, E., & Hill, A., 2002. The Petroleum Geology of South Australia: Volume 1. Otway Basin, chap. 6. Lithostratigraphy and Environments of Deposition, pp. 1–98, Department of Primary Industries and Resources South Australia.

Buckingham, I., 1992. Killara No. 1., Otway Basin, Victoria, Well Completion Report, Tech. rep., Anglo Australian Oil Company, N.L.

Cagniard, L., 1953. Basic theory of the magneto-telluric method of geophysical prospecting, Geophysics, 18(3), 605–635.

Caldwell, T. G., Bibby, H. M., & Brown, C., 2004. The magnetotelluric phase tensor, Geophysical Journal International, 158(2), 457–469.

Constable, S. C., Parker, R. L., & Constable, C. G., 1987. Occam's inversion: A practical algorithm for generating smooth models from electromagnetic sounding data, Geophysics, 52(3), 289–300.

de Graaf, B., Reid, I., Palmer, R., Jenson, D., & Parker, K., 2010. Salamander 1: a geothermal well based on petroleum exploration results, in Proceedings of the 2010 Australian Geothermal Energy Conference.

Geoscience Australia, 2014. Geoscience Australia Petroleum Well Database, http://dbforms.ga. gov.au/www/npm.well.search.

Geoscience Victoria, 2014. Geovic 3.0 well report, http://er-info.dpi.vic.gov.au/sd_weave/ anonymous.html.

Hart, B. S. & Balch, R. S., 2000. Approaches to defining reservoir physical properties from 3-D seismic attributes with limited well control: An example from the Jurassic Smackover Formation, Alabama, Geophysics, 65(2), 368–376.

Hillis, R. R., Monte, S., Tan, C., & Willoughby, D. R., 1995. The contemporary stress field of the Otway Basin, South Australia: implications for hydrocarbon exploration and production, The Australian Petroleum Production and Exploration Association Journal, 35, 494–506.

Hot Rock Ltd., 2009. Stratigraphic horizon interpretations for the Otway Basin, unpublished data.

Jensen-Schmidt, B.; Cockshell, C. & Boult, P., 2002. . The Petroleum Geology of South Australia: Volume 1. Otway Basin, chap. 5. Structural and tectonic setting, pp. 1–14, Department of Primary Industries and Resources South Australia.

Kirkby, A., Heinson, G., Holford, S. and Thiel, S., 2015, Mapping fractures using 1d anisotropic modelling of magnetotelluric data: a case study from the Otway Basin, Victoria, Australia, Geophysical Journal International, 201 (3), 1961-1976.

Kirkby, A., Heinson, G., and Krieger, L., 2016, Relating permeability and electrical resistivity in fractures using random resistor network models, Journal of Geophysical Research, accepted manuscript.

MacFarlane, J., Thiel, S., Pek, J., Peacock, J., & Heinson, G., 2014. Characterisation of induced fracture networks within an enhanced geothermal system using anisotropic electromagnetic modelling, Journal of Volcanology and Geothermal Research, 288, 1–7.

Morton, J., Sansome, A., & Boult, P., 2002. The Petroleum Geology of South Australia: Volume 1. Otway Basin, chap. 10. Reservoirs and seals, pp. 1–30, Department of Primary Industries and Resources South Australia.

Muñoz, G., 2014. Exploring for geothermal resources with electromagnetic methods, Surveys in Geophysics, 35(1), 101–122.

Nelson, E., Hillis, R., Sandiford, M., Reynolds, S., & Mildren, S., 2006. Present-day state-of-stress of Southeast Australia, The Australian Petroleum Production and Exploration Association Journal, 46(1), 283–305.

O'Neil, B., 2002. The Petroleum Geology of South Australia: Volume 1. Otway Basin, chap. 2. History of petroleum exploration and development, pp. 1–27, Department of Primary Industries and Resources South Australia.

Peacock, J. R., Thiel, S., Reid, P., & Heinson, G., 2012. Magnetotelluric monitoring of a fluid injection: Example from an enhanced geothermal system, Geophysical Research Letters, 39(18), 1–5.

Peacock, J. R., Thiel, S., Heinson, G., & Reid, P., 2013. Time-lapse magnetotelluric monitoring of an enhanced geothermal system, Geophysics, 78(3), B121–B130.

Pek, J. & Santos, F. A., 2006. Magnetotelluric inversion for anisotropic conductivities in layered media, Physics of the Earth and Planetary Interiors, 158(24), 139 – 158.

Pellerin, L., Johnston, J. M., & Hohmann, G. W., 1996. A numerical evaluation of electromagnetic methods in geothermal exploration, Geophysics, 61(1), 121–130.

Perincek, D. & Cockshell, C. D., 1995. The Otway Basin: early Cretaceous rifting to Neogene inversion, The Australian Petroleum Production and Exploration Association Journal, 35, 451–451.

Russell, B., Hampson, D., Schuelke, J., & Quirein, J., 1997. Multiattribute seismic analysis, The Leading Edge, 16(10), 1439–1443.

Ryan, S., Knight, L., & Parker, G., 1995. The stratigraphy and structure of the Tyrendarra Embayment, Otway Basin, Victoria, Victorian Initiative for Minerals and Petroleum Report 15, Department of Agriculture, Energy and Minerals.

Tassone, D., 2014. Compressional deformation and exhumation in sedimentary basins at 'passive' continental margins, with implications for hydrocarbon exploration and development. PhD Thesis, The University of Adelaide.

Tikhonov, A. N., 1950. On determining electrical characteristics of the deep layers of the Earth's crust, Doklady Akademii Nauk, 2, 295–297.

Ussher, G., Harvey, C., Johnstone, R., & Anderson, E., 2000. Understanding the resistivities observed in geothermal systems, in Proceedings of the World Geothermal Congress, pp. 1915–1920.

Vandenberg, A., 2000. The Tasman Fold Belt system in Victoria: geology and mineralisation of Proterozoic to Carboniferous rocks, Tech. Rep. Geological Survey of Victoria Special Publication, Department of Agriculture, Energy and Minerals, Victoria.

Wannamaker, P. E., 2005. Anisotropy versus heterogeneity in continental solid earth electromagnetic studies: Fundamental response characteristics and implications for physicochemical state, Surveys in Geophysics, 26(6), 733–765.

Wright, P. M., Ward, S. H., Ross, H. P., & West, R. C., 1985. State-of-the-art geophysical exploration for geothermal resources, Geophysics, 50(12), 2666–2696.